Anti-Cancer Drugs 2000, **11,** pp. 445–454

Report

FR901228 causes mitotic arrest but does not alter microtubule polymerization

Victor Sandor,[1,5] April R Robbins,[2] Rob Robey,[1] Tim Myers,[3] Edward Sausville,[3] Susan E Bates[1] and Dan L Sackett[3,4]

[1]Medicine Branch, National Cancer Institute, [2]Laboratory of Cell Biochemistry and Biology, National Institute of Diabetes, Digestive and Kidney Diseases, [3]DTP Clinical Trials Unit, Developmental Therapeutics Program, National Cancer Institute, [4]Laboratory of Integrative and Medical Biophysics, National Institute of Child Health and Human Development, National Institutes of Health, Bethesda, MD 20892, USA. [5]Present Address: Jewish General Hospital, Department of Oncology, Room E172, 3755 Cote St Catherine, Montreal, Quebec H3T 1E2, Canada.

FR901228, a natural cyclic depsipeptide, shows high cytotoxicity against human cancer cell lines (low nM IC_{50} values). Cells exposed to FR901228 arrest with G_1 or G_2/M DNA content; S phase is depleted. G_2/M cells include cells arrested in mitosis. We wished to understand the mitotic arrest by this compound. Mitotic arrest is often due to interference with microtubules and COMPARE testing in the NCI drug screen indicated a possible taxane-like mechanism. Testing of FR901228 for tubulin binding or alteration of *in vitro* MT assembly failed to reveal any effect. Likewise, examination of cellular microtubules following exposure to FR901228 did not reveal any change. Similar G_2/M accumulation was observed in MCF7, MCF10 and PC3 cells. About 50% of G_2/M cells were mitotic and contained microtubule spindles. Mitotic cells peaked at about 14–16 h drug exposure and declined to near 0% by 24–30 h. The block was at prometaphase, with numerous chromosomes unattached to the spindle. We conclude that FR901228 induces formation of aberrant spindles probably by interfering with chromosome attachment, causing mitotic accumulation without affecting mitotic microtubules.

Key words: Histone deacetylase inhibitors, microtubules, mitosis, prometaphase.

Introduction

Current classes of antineoplastic agents offer limited therapeutic benefits for most human malignancies. Thus, identification and development of new agents with novel mechanisms of action are priorities for improving cancer therapeutics. While empirical evaluation of clinical efficacy remains the cornerstone for the clinical development of novel agents, an understanding of the mechanism of action of putative new antineoplastic agents is important for the development of rational strategies for both selection of compounds for clinical development and optimization of clinical use.

FR901228 is a cytotoxic cyclic depsipeptide isolated by the Fujisawa Pharmaceutical Company from the fermentation broth of *Chromobacterium violaceum*.[1] Initial characterization of this compound showed it to be cytotoxic at nanomolar concentrations in several *in vitro* and *in vivo* models.[2] In H-*ras* transformed NIH 3T3 cells, FR901228 was found to cause a G_1 cell cycle arrest and to down-regulate c-*myc* mRNA expression.[3] In human MCF-7 transformants, FR901228 was reported to cause a G_1 and a G_2/M arrest.[4] This agent has shown *in vitro* activity against human leukemia[5] and human breast cancer cells.[6] Interest in this compound was generated by its potency and potential as an antineoplastic agent with a novel mechanism of action involving growth regulation. FR901228 is currently undergoing phase I testing.

A complete understanding of the mechanism of action of this novel compound is not yet at hand, although it has been demonstrated to inhibit histone deacetylase activity.[4] To further characterize the mechanism of action of FR901228 and to identify compounds with potentially similar mechanisms of action, we performed a COMPARE analysis using the NCI Anticancer Drug Screen database with FR901228 as a seed. This analysis utilizes the cytotoxicity data derived from screening compounds against the 60 cell

Correspondence to DL Sackett, Building 12A, Room 2041, NIH, 12 South Drive, MSC 5626, Bethesda, MD 20892-5626, USA.
Tel: (+1) 301 594-0358; Fax: (+1) 301 496-2172;
E-mail: sackettd@mail.nih.gov

lines of the NCI Anticancer Drug Screen. The patterns of cytotoxicity are compared with those of previously tested compounds in order to identify similarities in action of the test compound to known reference compounds. The ability of COMPARE to group compounds with similar mechanisms of action, similar molecular targets or similar mechanisms of resistance has been previously demonstrated.[7,8] COMPARE revealed a significant correlation between FR901228 and taxanes. Pursuing this correlation, we examined the effects of FR901228 on tubulin and microtubules, and investigated the G_2/M block induced by this compound.

Material and methods

Cell lines and cell culture

PC3 and MCF-7 cells were obtained from the National Cancer Institute Anticancer Drug Screen. Cells were grown in RPMI medium (Biofluids, Rockville, MD) containing 10% fetal bovine serum (Gibco/BRL, Grand Island, NY). MCF-10A is an immortalized EGF-dependent breast cell line kindly provided by Dr David Salomon (NIH, Bethesda, MD).[9] MCF-10A cells were maintained in DMEM/F12 medium (Biofluids) with 5% horse serum (Gibco/BRL), 10 ng/ml human EGF (Upstate Biotechnology, Lake Placid, NY), 500 ng/ml hydrocortisone (Sigma, St Louis, MO) and 10 μg/ml bovine insulin (Sigma).

COMPARE analysis

The NCI Anticancer Drug Screen measures cytotoxicity and growth inhibition in an assay using 60 human tumor cell lines. The GI_{50} endpoint is a time zero corrected IC_{50} and is defined as the concentration of an agent that causes 50% growth inhibition. An activity pattern comprised of 60 GI_{50} values is obtained for the tested compound. A COMPARE search using a 'seed' compound of interest produces a list of compounds ('hits') having the most similar patterns of activity. The structure and known biological activity of the 'hits' are used to develop hypotheses about the seed's mode of cytotoxicity/growth inhibition. These activity pattern correlations have been predictive for several mechanisms of action classes including antimitotics,[10] thioredoxin inhibitors[11] and, most recently, inhibitors of cyclin-dependent protein kinases.[12] For activity patterns that demonstrate a strong correlation with MDR phenotype (measured as either levels of MDR1 mRNA or functionally as rhodamine exclusion), it is useful to run a COMPARE search using only the subset of cell lines that do not have the MDR phenotype. The cell lines excluded in this study were: HOP-62, SW-620, DLD-1, HCT-15, NCI/ADR-RES, CCRF-CEM, UO-31, A498, CAK1, RXF-393, ACHN and SF-295. The COMPARE program and activity pattern database used were essentially the same as those accessible via the NCI Developmental Therapeutics Program website (http://dtp.nci.nih.gov).

Immunocytochemistry

Cells cultured in chamber slides and subject to treatment as indicated in the figures were fixed by immersion in absolute methanol at -20°C for 10 min. Slides were subsequently washed with phosphate-buffered saline (PBS) (Biofluids) and blocked with blocking buffer containing 4% BSA in PBS for 10 min at room temperature. Slides were incubated with mouse monoclonal anti-α-tubulin antibody (Sigma) diluted 1:200 in blocking buffer for 1 h, washed 3 times with PBS, then stained for 1 h with FITC-labeled anti-mouse antibody (Vector, Burlingame, CA) diluted 1:500 in blocking buffer. The slides were washed again with PBS, mounted with Fluoromount G and analyzed with standard or confocal fluorescence microscopy as indicated in the figures. Mitotic index was evaluated following staining with the DNA dye Hoechst 33258. Cells were grown on two-chamber coverglass slides for 48 h prior to drug treatment. Following drug addition, Hoechst 33258 was added to the medium to a final concentration of 5 μg/ml 90 min prior to each time point. Fluorescent images were captured from non-overlapping fields and 400–500 cells were quantitated for each time point using the Cavalieri macro of NIH Image.

Tubulin binding and polymerization assays

Microtubule protein [MTP, consisting of tubulin and microtubule association proteins (MAPs)] was isolated from frozen rat brains as previously described.[13] Tubulin was purified from this MTP preparation by selective polymerization as described.[14] Concentrated solutions of tubulin and MTP in MME buffer (0.1 M morpholinoethansulfonic acid, 1 mM $MgCl_2$, 1 mM ethyleneglycol-bis-tetraacetic acid, pH 6.9) were drop frozen in liquid nitrogen and stored in liquid nitrogen until use. Polymerization was monitored by following the optical density at 350 nm of a 0.25 ml solution of tubulin or MTP in MME buffer with 1 mM GTP. Assays were performed with a thermostated Cary 219. Binding to the tubulin dimer was assayed in two ways. Changes in the intrinsic fluorescence of tubulin due to drug binding[15] were monitored using a Perkin-Elmer LS-50B spectrofluorometer. Excitation was at

280 nm and emission was monitored from 290 to 400 nm. Perturbation of tubulin sulfhydryls was evaluated using the reaction with dithionitrobenzoic acid (DTNB). DTNB was added to a final concentration of 120 μM to a solution of 4 μM tubulin without or with drug preincubation and sulfhydryl reaction was monitored at 412 nm.

Flow cytometry and cell cycle analysis

Exponentially growing cells (50–70% confluent) were harvested by trypsinization, washed twice with PBS and resuspended in cold 75% ethanol in PBS, and kept at 4°C for at least 30 min. Prior to analysis, cells were washed with PBS, and resuspended and incubated for 30 min in propidium iodide staining solution containing 0.05 mg/ml propidium iodide (Sigma), 1 mM EDTA, 0.1% Triton X-100 and 1 mg/ml RNase A in PBS. The suspension was then passed through a nylon mesh filter and analyzed on a FACSort flow cytometer (Becton Dickinson, San Jose, CA). ModFiltLT version 2.0 (Verify Software, Topsham, ME) was used to determine the percentage of cells in each phase of the cell cycle.

Mitotic cells were quantitated by bivariate flow analysis using propidium iodide and the mitotic antibody TG3[16] (kind gift of Dr Peter Davies, Albert Einstein College of Medicine). Trypsinized, washed cells were resuspended in 500 μl of RPMI and 500 μl of fetal calf serum and 3 ml of ice-cold 70% ethanol solution was added dropwise. The cells were allowed to incubate for at least 30 min at 4°C, after which they were centrifuged and resuspended in blocking solution (2% BSA in PBS) and allowed to incubate overnight at 4°C. The cells were then centrifuged and resuspended in blocking solution with TG3 antibody (hybridoma cell culture medium), diluted 1:10 and allowed to incubate for 30 min. After washing with blocking solution, the cells were stained with FITC-conjugated goat anti-mouse secondary antibody for 30 min. To determine DNA content, the cells were then centrifuged and resuspended in 450 μl PBS, 450 μl of propidium iodide solution (50 μg/ml in PBS) and 50 μl RNase solution (5 mg/ml in PBS), and allowed to incubate for 30 min. FITC fluorescence was monitored with a 525 nm bandpass filter and propidium iodide with a 585 nm bandpass filter.

Results

FR901228 (NSC 630176) was among the many compounds that were predicted by COMPARE analysis (see Methods for details) to be MDR substrates and then confirmed as such in independent assays. In a previous study, a pattern composed of the levels of functional P-glycoprotein expression in the 60 cell lines of the NCI Anticancer Drug Screen was used as a 'seed' in a COMPARE search for correlated cytotoxicity patterns. Compounds having patterns of cytotoxic potency negatively correlated with P-glycoprotein function were hypothesized to be substrates for the multidrug transporter.[17] This hypothesis was validated for multiple compounds.

More recently, FR901228 itself was used as a seed in a COMPARE search for compounds having the same activity pattern. Among those most similar were a large number of taxane analogs, as well as a number of confirmed substrates for the P-glycoprotein efflux pump (e.g. bisantrene). This implied that the correlations between the 'seed' and the COMPARE hits might not be independent of the MDR effect. To remove the MDR effect, only non-MDR cell lines were used for the next COMPARE search using FR901228 as a 'seed'. Reproduced in Table 1, the non-MDR COMPARE result shows taxane analogs were still the most frequent structure type in the list of similar compounds (eight of 15). Figure 1 presents the structures of FR901228 and of five of the eight taxanes. Pursuing this correlation, the ability of FR901228 to modulate microtubule function both *in vitro* with purified tubulin and in whole cells was investigated.

In vitro assays of the effects of FR901228 on tubulin polymerization are shown in Figure 2(A and B). Tubulin dimers can be driven to polymerize *in vitro* by various agents including the addition of MAPs and GTP or the addition of paclitaxel. Polymerization can

Table 1. Summary of compounds with high correlation after removal of P-glycoprotein

NSC	Compound type	Pearson	
		All 60	No MDR lines
630176	FR901228	1	1
6002223	[Taxane]	0.757	0.641
600220	[Taxane]	0.763	0.61
600221	[Taxane]	0.746	0.633
643915		0.472	0.597
649941		0.437	0.595
703097		0.369	0.573
671871	[Taxane]	0.745	0.567
699091		0.41	0.56
125973	Taxol	0.693	0.55
662161	[Taxane]	0.642	0.542
626868		0.421	0.541
671872	[Taxane]	0.723	0.539
700268		0.216	0.526
375504		0.404	0.526
689291	[Taxane]	0.728	0.518

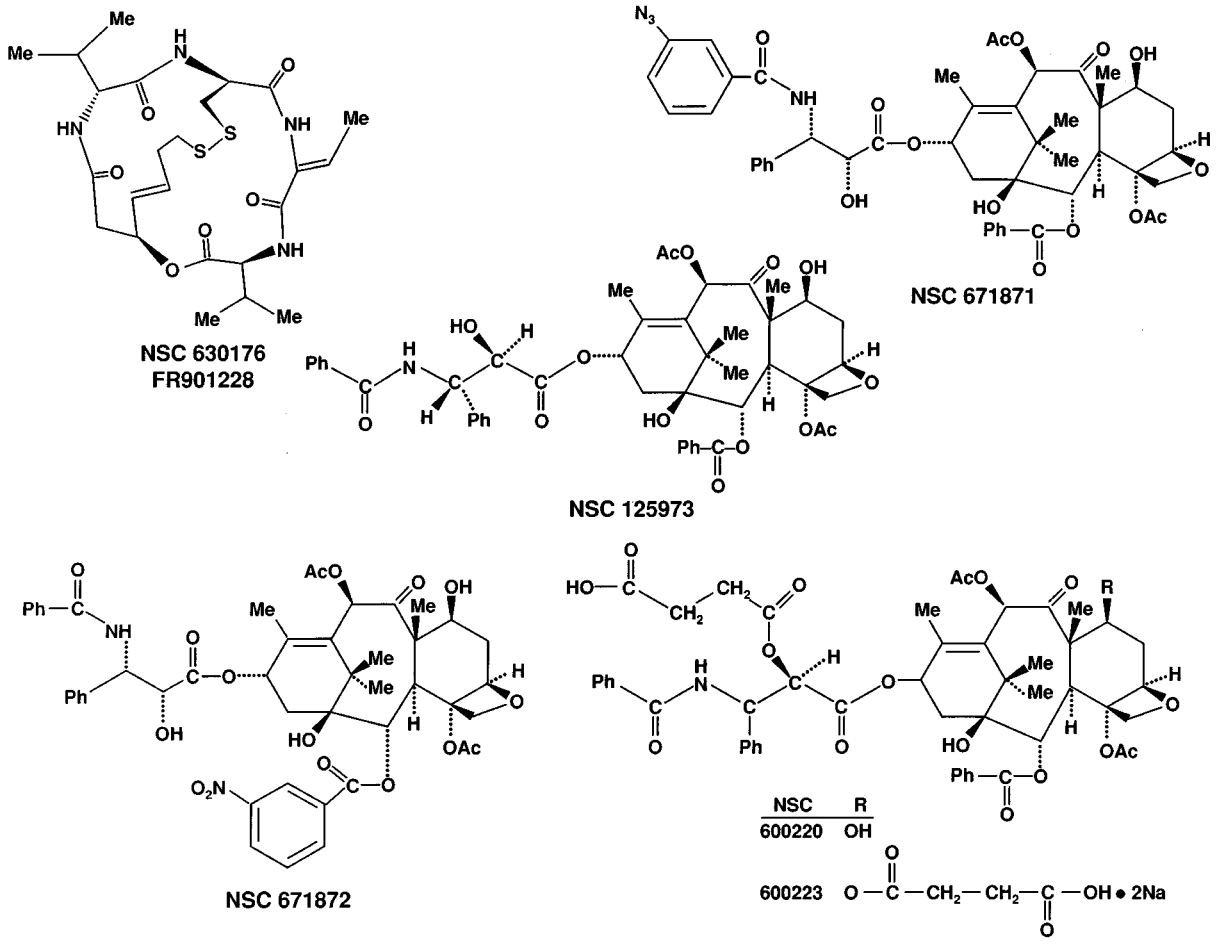

Figure 1. Chemical structures of FR901228, paclitaxel and high correlation taxanes.

be quantified by variations in the turbidity of the solution, which increases as tubulin polymers form. Exposure to cold causes the rapid depolymerization of tubulin and a decrease in turbidity. This effect is dampened by paclitaxel which stabilizes polymerized microtubules. Figure 2(A and B) shows that at a concentration of 50 μM FR901228 had no effect on the ability of tubulin to polymerize *in vitro* when driven by MAPS and GTP or by paclitaxel. In addition, FR901228 was without significant effect on the stability of polymerized microtubules exposed to cold.

It is possible that FR901228 binds to tubulin but induces changes too subtle to detect in the polymerization assays just described. Hence we evaluated the direct interaction of FR901228 with unpolymerized tubulin. Tubulin dimers contain eight tryptophan residues. Binding of various drugs to tubulin, such as colchicine or maytansine, has been shown to quench the fluorescence emission of tubulin.[15] Figure 2(C) shows the emission spectrum of tubulin alone, in the presence of colchicine, maytansine or FR901228. Both of the known tubulin binding agents quenched the emission spectrum of tubulin as expected. In contrast, FR901228 at 50 mM did not alter the emission spectrum suggesting that FR901228 does not bind to tubulin near these tryptophan residues and does not conformationally alter tubulin so as to quench the emission spectrum caused by these residues.

The tubulin dimer contains 20 reduced sulfhydryls. These groups are all exposed and reactive in the unpolymerized dimer, and the kinetics of reaction are sensitive to drug binding near these sites. Colchicine analogs, podophyllotoxin, vincristine, maytansine and paclitaxel all decrease the kinetics of reaction of tubulin with the sulfhydryl reactive compound DTNB (data for maytansine only are shown in Figure 2D). FR901228 at a concentration of 50 μM did not significantly alter the kinetics of DTNB reaction or the yield of reactive sulfhydryl groups (Figure 2D). Taken together with the emission spectrum data above, it appears highly unlikely that FR901228 binds directly to tubulin dimers.

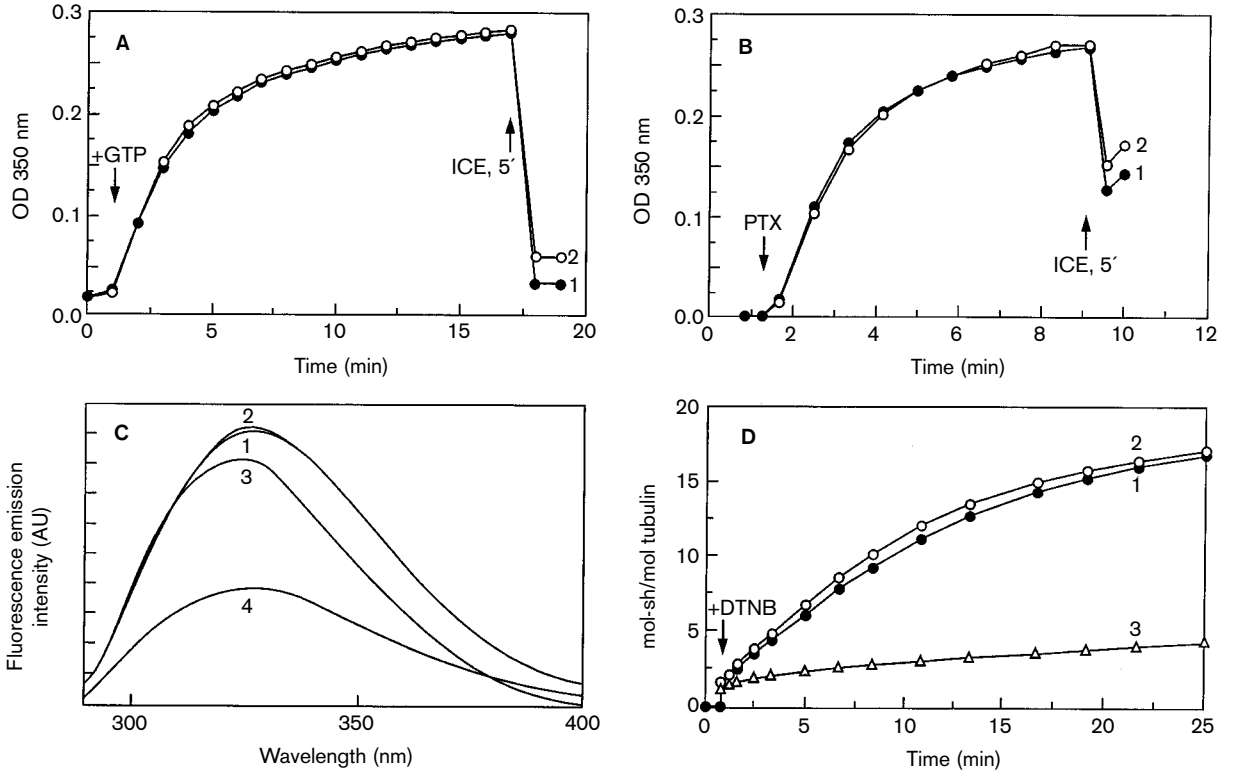

Figure 2. FR901228 effects on tubulin polymerization and binding assays. Tubulin polymerization was induced by (A) MAPS and GTP or (B) paclitaxel (PTX). (A) MAP-containing tubulin (MTP) at 1.4 mg/ml in MME buffer was induced to polymerize by addition of 1 mM GTP at the time indicated. The solution contained no addition (1) or 50 μM FR901228 (2). Depolymerization was induced by incubation on ice for 5 min at the time indicated. (B) MAP-free tubulin, 1 mg/ml in MME+0.4 mM GTP was induced to polymerize by addition of 10 μM PTX at the time indicated. Partial depolymerization was induced by incubation on ice for 5 min at the time indicated. (1) Control and (2) 50 μM FR901228. Binding to tubulin was assessed by (C) effects on tubulin fluorescence and (D) changes in sulfhydryl reactivity. (C) The fluorescence emission of 0.5 mg/ml tubulin (5 μM) was monitored following excitation at 280 nm. Solutions were preincubated with (1) no addition, (2) 40 μM FR901228, (3) 8 μM maytansine and (4) 9 μM colchicine. The tubulin–colchicine complex was prepared at higher concentration and diluted, as described.[24] (D) The reactivity of tubulin sulfhydryls was assessed by the addition at the time indicated of 120 μM DTNB (final concentration) to a solution of 4 μM tubulin in MME buffer. The solutions contained (1) no addition, (2) 50 μM FR901228 or (3) 25 μM maytansine. The reaction was monitored by changes in absorbance at 412 nm. All samples yielded the expected 20 mol of SH/mol of tubulin when samples were made 2 M in guanidine hydrochloride at 30 min (data not shown).

It is possible that an agent could interfere with microtubule function by binding to a protein other than tubulin. Therefore, the ability of FR901228 to alter interphase microtubules *in vivo* was investigated using immunofluorescence in MCF-10A cells. These cells were chosen because their highly spread phenotype facilitated examination of the microtubule array; similar results were found with MCF-7 and PC-3 cells (results not shown). Interphase microtubules were stained with anti-α-tubulin antibody after exposure to 10 ng/ml of FR901228 for 18 h and compared to untreated cells and cells treated with 100 ng/ml paclitaxel for 18 h. Figure 3(A, C and E) shows representative images from untreated, FR901228-treated and paclitaxel-treated cells. While paclitaxel caused characteristic microtubule bundling and aster formation, FR901228 caused no appreciable changes in interphase microtubule structure. The ability of FR901228 to stabilize microtubules was further investigated by assessing its ability to cold-stabilize microtubules. Untreated cells, cells treated with FR901228 10 ng/ml and cells treated with paclitaxel 100 ng/ml were placed on ice for 30 min prior to fixation in order to induce microtubule depolymerization. Representative images obtained following immunostaining are shown in Figure 3(B, D and F, respectively). While cells treated with paclitaxel showed persistent microtubule bundling, cells treated with FR901228 were indistinguishable from the untreated cells and showed a ground-glass pattern of staining indicative of cytoplasmic depolymerized tubulin dimers. Similar results were found

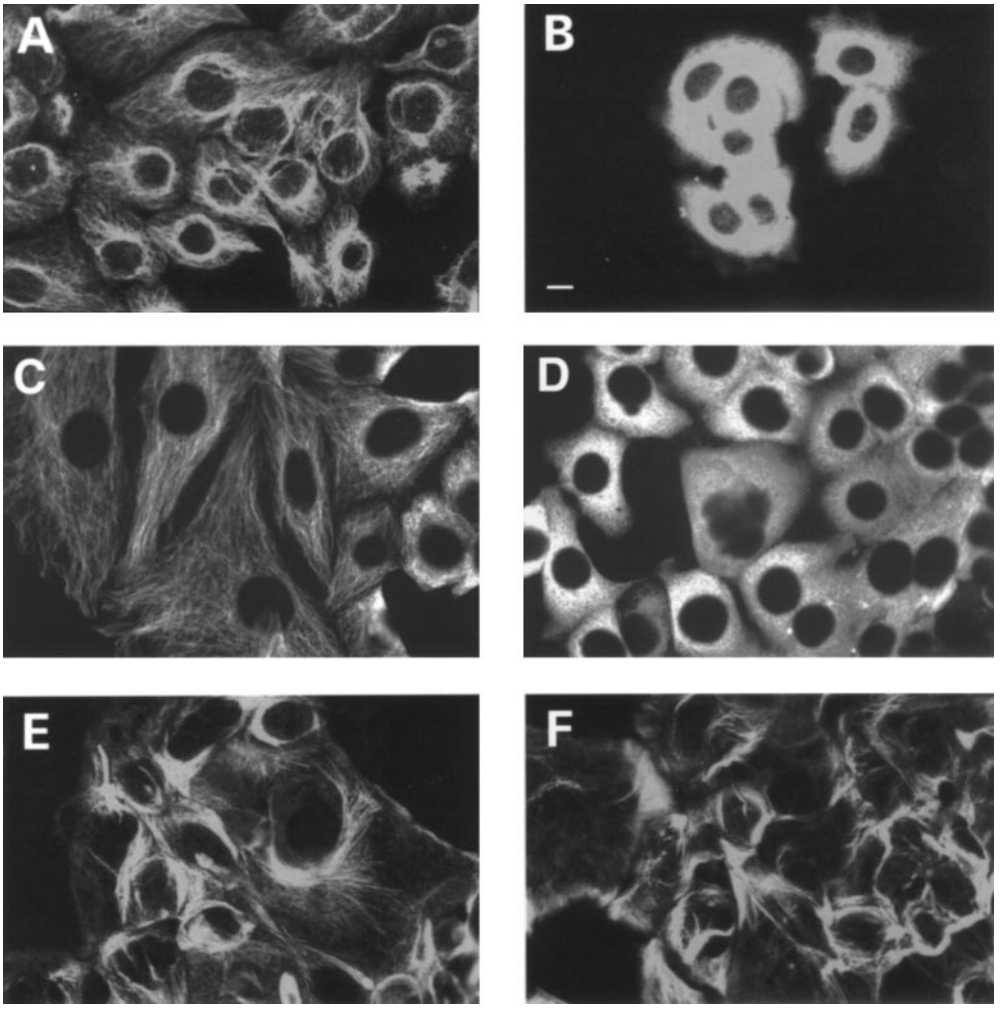

Figure 3. Effects of FR901228 on cellular microtubules. MCF7 cells were treated for 18 h with paclitaxel or FR901228 and then kept at 37°C or exposed to ice for 30 min prior to fixation and immunostaining for microtubules. (A, C and E) Cells kept warm. (B, D and F) Cells exposed to ice for 30 min. (A and B) Controls. (C and D) Cells treated with FR901228, 10 ng/ml for 18 h. (E and F) Cells treated with paclitaxel, 100 ng/ml for 18 h. The bar in (B) represents 10 μm.

with higher concentrations of FR901228 (not shown).

Finding no evidence to support the hypothesis that FR901228 and taxanes affect the same molecular target(s), we next asked whether they had similar effects on cell cycle progression. Figure 4 shows DNA cell cycle histograms for three cell lines: MCF-7, PC-3 and MCF-10. In all three cell lines, both a G_1 and a G_2/M arrest were evident after treatment with FR901228, 10 ng/ml for 18 h. FR901228 does not appear to block S phase progression, so the G_1 and G_2/M arrests are accompanied by a loss of cells in S phase.

In order to characterize more precisely the G_2/M arrest caused by FR901228, the mitotic index was determined in all three cell types over a time course of exposure to the drug. This was done by microscope counts after bisbenzamide staining (not shown) and by bivariate flow cytometry using propidium iodide to quantitate DNA and the mitosis-specific antibody TG3[16] to quantitate cells in mitosis. Both methods demonstrated that a significant mitotic block was induced. Figure 5 presents the results of flow cytometry performed with MCF7 cells after varying times of exposure to 10 ng/ml of FR901228. The accumulation of cells in G_1 and G_2/M at the expense of S phase is evident by 12 h and definite by 24 h. At 12 h, many of the G_2/M cells are blocked in mitosis, evidenced by the significant increase in the $TG3^+$ cells; by 24 h, all mitotic cells were gone. The complete time course is shown in the graph, indicating that at their peak mitotic cells constituted about 50% of the

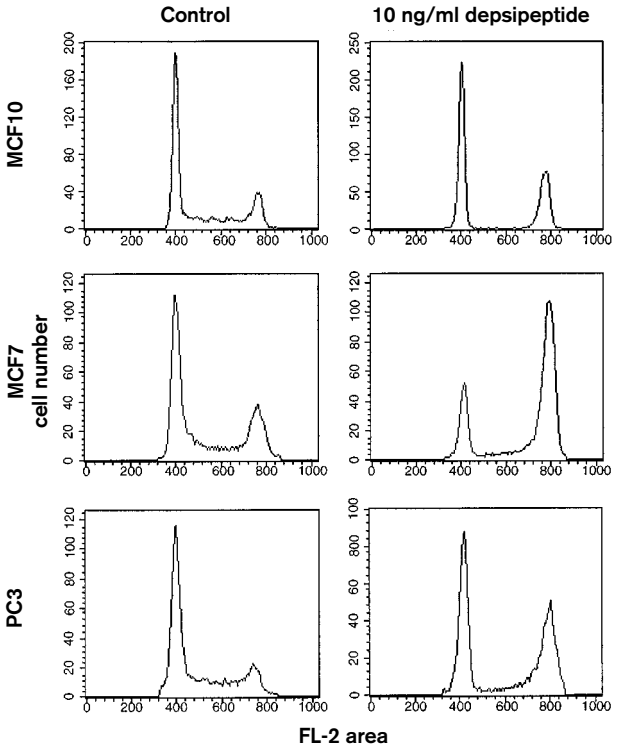

Figure 4. Cell cycle results. Flow cytometric analysis of DNA content of PC3, MCF7 and MCF10 cells with and without 20 h treatment with FR901228. Cells were treated with drugs and processed for propidium iodide staining and flow cytometry as outlined in Materials and methods. In all three cell lines, a significant increase is observed in the fraction of cells with G_2/M content of DNA following drug exposure. All three lines also show a significant loss of cells in S phase.

G_2/M population. PC3 cells showed a similar rise and fall of mitotic index with time of exposure to FR901228; however, no increase in mitotic cells was found with MCF10A cells exposed to the drug.

The maximal extent of mitotic accumulation was variable and found to depend on the cell density at the time of exposure to the drug. Higher cell densities resulted in lower maximal mitotic indexes. A similar sensitivity to cell density was found in the ability of trichostatin A, like FR901228 an inhibitor of histone deacetylase activity, to induce or suppress gene expression in Hep 3B cells.[18]

Cells blocked in mitosis can be arrested at different stages of this complex process. The nature of the mitotic arrest observed in MCF-7 and PC-3 cells was examined by immunofluorescence microscopy after FR901228 exposure. Figure 6(A) shows a field of MCF-7 cells after incubation for 12 h with FR901228. Staining of DNA with DAPI revealed one prophase (small arrow) and 10 prometaphase cells; the latter are characterized by condensed chromosomes scattered about the cytoplasm. The lower panels show, at higher magnification, the mitotic spindles, stained with anti-tubulin (Figure 6B), and condensed chromosomes stained with DAPI (Figure 6B′) in two FR901228-treated cells. Both cells display chromosomes outside the spindles (arrows in Figure 6B′). These results indicate that, although the microtubule spindle forms, there is some block that interferes with formation of the proper contacts between all chromosomes and the microtubule spindle fibers.

Discussion

COMPARE analysis using the NCI Anticancer Drug Screen database has been previously demonstrated to be able to establish a compound as having a similar mechanism of action to other compounds in the database.[7,8] COMPARE analysis using FR901228 as a seed compound indicated a high and statistically significant correlation to the taxanes, suggesting tubulin or microtubules as a likely target of this compound.[10] However, results of experiments presented above gave no evidence of interaction between FR901228 and these targets.

Cell cycle analysis demonstrated that FR901228 causes a G_2/M arrest similar to the taxanes, as well as the previously reported G_1 cell cycle arrest. In addition, the mitotic index of PC3 and MCF-7 cells treated with FR901228 increased to a maximum after about 12–15 h of treatment. Examination of the morphology of these mitotic cells demonstrated abnormal spindle formation and function. The mitotic cells, however, constituted 50% or less of the population of cells determined to be in G_2/M by propidium iodide staining and flow cytometry. The immortalized normal breast epithelium cell line, MCF-10A, showed no mitotic arrest after FR901228 exposure.

Recently it was reported that FR901228 inhibits histone deacetylase.[4] Other histone deacetylase inhibitors have been shown to cause both a G_1 and G_2/M arrest; the mechanism by which this occurs remains to be elucidated. Our data characterizes the G_2/M arrest as a prometaphase arrest in PC3 and MCF-7 cells as well as demonstrating a G_2 block in these and other cells (MCF10). It is known that entry into metaphase and progression through anaphase requires the complete and proper alignment of chromosomes along the metaphase plate.[19,20] Disruption of this process at any point after CDK-1 activation will arrest cells prior to metaphase. Mitotic arrest caused by taxanes is a prometaphase arrest, characterized by

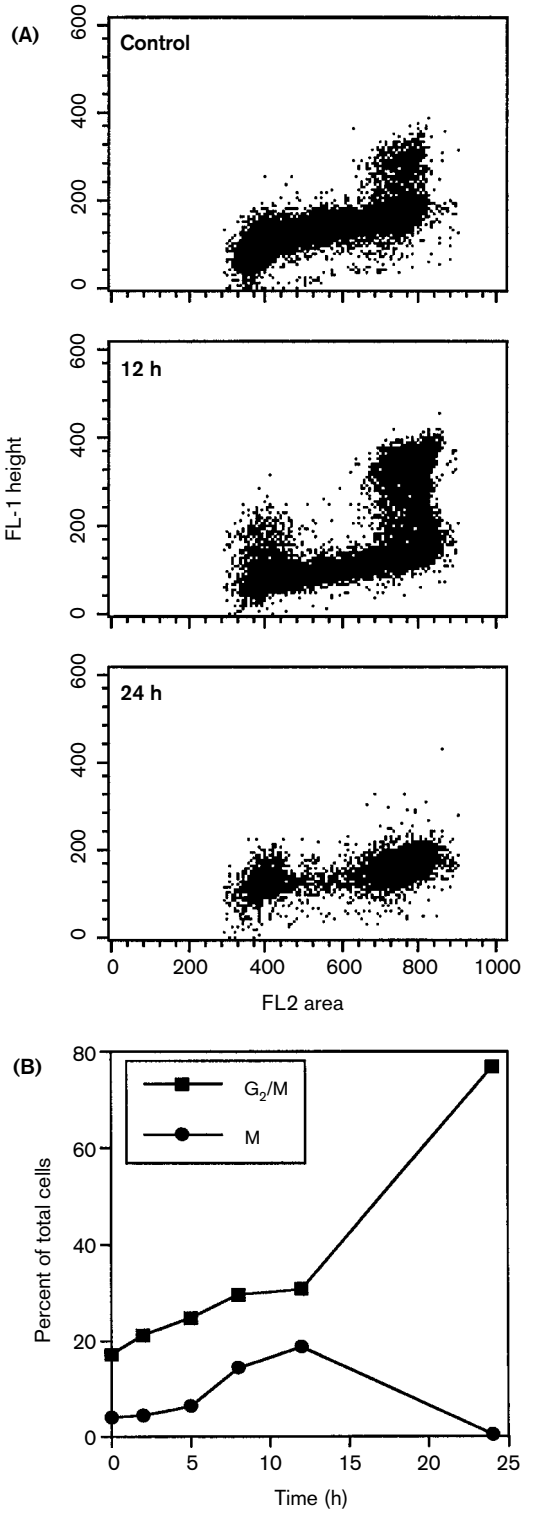

Figure 5. Two-parameter FACS after various times of exposure. MCF7 cells were exposed to 10 ng/ml FR901228 for various times and then processed for flow cytometry using propidium iodide to measure DNA content and TG-3 antibody labeling to measure mitotic cells. (A) Two-parameter plots are shown for control (no drug), and for 12 and 24 h exposure. (B) Results from a series of time points, including those in (A), are presented. The G_2/M numbers are from the propidium iodide data and the mitotic (M) numbers represent the G_2/M cells that are also TG-3$^+$.

formation of an incomplete metaphase plate.[21] In this respect, FR901228 and the taxanes share a common mechanism and site for cell cycle disruption, and presumably for the triggering of cell death pathways.

The cell cycle arrest seen in MCF-10A cells differs substantially from that seen in PC3 and MCF-7 cells in that no mitotic figures are observed. In addition, and

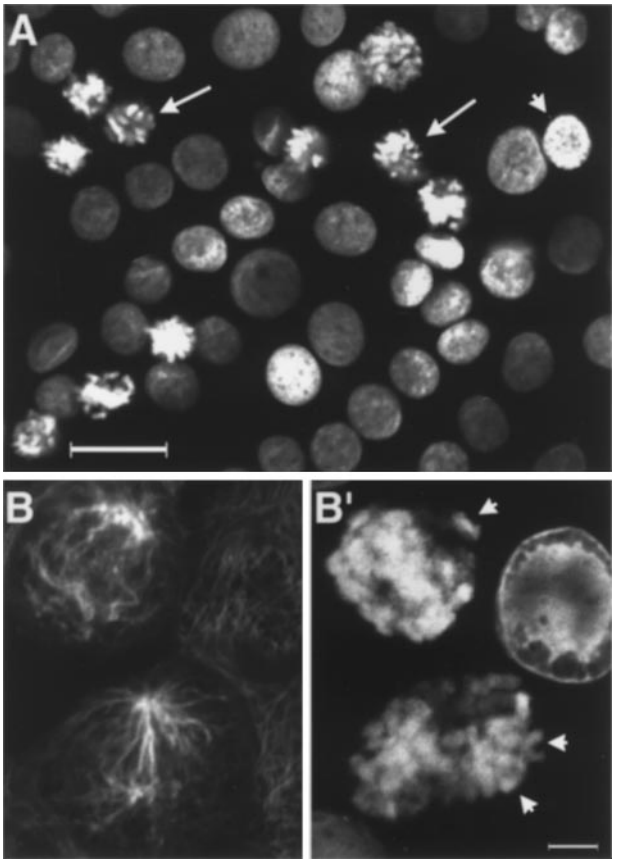

Figure 6. Aberrant mitotic figures following exposure to FR901228. MCF7 cells were stained following drug exposure in order to reveal mitotic figures. (A) Live cells were stained following 12 h exposure to 10 ng/ml FR901228. Hoechst 33258 (final 5 μg/ml) was added to the growth medium 1.5 h prior to imaging. Long arrows indicate two of the 10 prometaphase cells present in this field. The short arrow indicates a prophase cell. Bar=25 μm. (B and B′) Cells were treated with drug for 13 h and then stained for (B) tubulin immunofluorescence with mouse anti-α-tubulin monoclonal DM1A or (B′) DNA with DAPI (4,6-diamidino-2-phenylindole, 1 μg/ml). Two prometaphase cells are present in the left side of the images. The short arrows in (B′) indicate mitotic chromosomes located outside of the mitotic spindle in each of these two cells. Bar=5 μm.

unlike the case in PC3 or MCF7 cells, CDK-1 activity is decreased and there is no accumulation of cyclin B (data not shown). These features indicate an arrest prior to the G_2 to M transition. This block is also observed in PC3 and MCF7 cells (since about 50% of the G_2/M cells are non-mitotic), in addition to the mitotic block. This effect is not mediated by p53 status alone as both MCF-10 and MCF-7 cells have a wild-type p53 status while PC3 cells are $p53^{null}$. Relaxed cell cycle arrest and propagation of unrepaired chromosomal damage have been previously reported in cancer cell lines with wild-type p53.[22] As MCF-10 cells are immortalized normal breast epithelial cells, their cell cycle checkpoint apparatus may be more intact than that of the malignant cell lines and, therefore, may be more readily triggered by the effects of FR901228.

A number of drugs have been shown to cause G_2/M cell cycle arrest through a variety of different mechanisms including: DNA damage, protein kinase C inhibition, inhibition of protein synthesis or protein degradation, histone deacetylase inhibition, CDK inhibition and microtubule disruption.[23] Despite this array of potential mechanisms, COMPARE identified taxanes as most highly correlated with FR901228 cytotoxicity; histone deacetylase inhibitors were not highly correlated. This might imply that, as with many other natural products, FR901228 has multiple cellular targets including but not limited to histone deacetylase inhibition. On the other hand, FR901228 has among the lowest IC_{50} of known histone deacetylase inhibitors. Thus, it may be the case that additional cellular targets are a feature of the cytotoxicity of these other agents, at their higher concentrations. It is our conclusion that a significant target for the cytotoxic effect of FR901228 is that involved in mediating an arrest in G_2 alone or in G_2 and in M. We are investigating the factors influencing these different arrest points. Given the potency and efficacy of other anticancer agents to induce G_2/M arrest, FR901228 is a potentially important new agent for cancer treatment. Further studies will be aimed at understanding its mechanism of action and the development of strategies for its clinical use.

References

1. Ueda H, Nakajima H, Hori Y, *et al*. FR901228, a novel antitumor bicyclic depsipeptide produced by *Chromobacterium violaceum* No. 968. I. Taxonomy, fermentation, isolation, physico-chemical and biological properties, and antitumor activity. *J Antibiot* 1994; **47**: 301–10.
2. Ueda H, Manda T, Matsumoto S, *et al*. FR901228, a novel antitumor bicyclic depsipeptide produced by *Chromobacterium violaceum* No. 968. III. Antitumor activities on experimental tumors in mice. *J Antibiot* 1994; **47**: 315–23.
3. Ueda H, Nakajima H, Hori Y, Goto T, Okuhara M. Action of FR901228, a novel antitumor bicyclic depsipeptide produced by *Chromobacterium violaceum* No. 968, on H-*ras* transformed NIH3T3 cells. *Biosci Biotech Biochem* 1994; **58**: 1579–83.
4. Nakajima H, Kim YB, Terano H, Yoshida M, Horinouchi S. FR901228, a potent antitumor antibiotic, is a novel histone deacetylase inhibitor. *Exp Cell Res* 1998; **241**: 126–33.
5. Byrd JC, Shinn C, Ravi R, *et al*. Depsipeptide (FR901228): a novel therapeutic agent with selective, in vitro activity against human B-cell chronic lymphocytic leukemia cells. *Blood* 1999; **94**: 1401–8.
6. Rajgolikar G, Chan KK, Wang H-CR. Effects of a novel antitumor depsipeptide, FR901228, on human breast cancer cells. *Breast Cancer Res Treat* 1998; **51**: 29–38.
7. Boyd MR, Paull KD. Some practical considerations and applications of the National Cancer Institute *in vitro* anticancer drug discovery screen. *Drug Dev Res* 1995; **34**: 91–109.
8. Bates SE, Fojo AT, Weinstein JN, *et al*. Molecular targets in the National Cancer Institute drug screen. *J Cancer Res Clin Oncol* 1995; **121**: 495–500.
9. Ciardiello F, Kim N, McGeady ML, *et al*. Expression of transforming grown factors alpha (TGF alpha) in breast cancer. *Ann Oncol* 1991; **2**: 169–82.
10. Paull KD, Lin CD, Malspeis L, Hamel E. Identification of novel antimitotic agents acting at the tubulin level by computer-assisted evaluation of differential cytotoxicity data. *Cancer Res* 1992; **52**: 3892–900.
11. Kunkel MW, Kirkpatrick DL, Johnson JI, Powis G. Cell line-directed screening assay for inhibitors of thioredoxin reductase signaling as potential anti-cancer drugs. *Anti-Cancer Drug Des* 1997; **12**: 659–70.
12. Zaharevitz DW, Gussio R, Leost M, *et al*. Discovery and initial characterization of the paullones, a novel class of small-molecule inhibitors of cyclin-dependent kinases. *Cancer Res* 1999; **59**: 2566–9.
13. Sackett DL, Knipling L, Wolff J. Isolation of microtubule protein from mammalian brain frozen for extended periods of time. *Prot Expression Purif* 1991; **2**: 390–3.
14. Wolff J, Knipling L, Sackett DL. Charge-shielding and the paradoxical stimulation of tubulin polymerization by guanidine hydrochloride. *Biochemistry* 1996; **35**: 5910–20.
15. Sackett DL. Vinca site agents induce structural changes in tubulin different from and antagonistic to changes induced by colchicine site agents. *Biochemistry* 1995; **34**: 7010–9.
16. Andersson HJ, deJong G, Vincent I, Roberge M. Flow cytometry of mitotic cells. *Exp Cell Res* 1998; **238**: 498–502.
17. Lee JS, Paull K, Alvarez M, *et al*. Rhodamine efflux patterns predict P-glycoprotein substrates in the National Cancer Institute drug screen. *Mol Pharmacol* 1994; **46**: 627–38.

18. Gray SG, Ekstrom TJ. Effects of cell density and trichostatin A on the expression of *HDAC1* and $p57^{Kip2}$ in Hep 3B cells. *Biochem Biophys Res Commun* 1998; **245**: 423–7.
19. Rieder CL, Khodjakov A. Mitosis and checkpoints that control progression through mitosis in vertebrate somatic cells. *Prog Cell Cycle Res* 1997; **3**: 301–12.
20. Rieder CL, Schultz A, Cole R, Sluder G. Anaphase onset in vertebrate somatic cells is controlled by a checkpoint that monitors sister kinetochore attachment to the spindle. *J Cell Biol* 1994; **127**: 1301–10.
21. Jordan MA, Toso RJ, Thrower D, Wilson L. Mechanism of mitotic block and inhibition of cell proliferation by taxol at low concentrations. *Proc Natl Acad Sci USA* 1993; **90**: 9552–6.
22. Olivier M, Bautista S, Valles H, Theillet C. Relaxed cell-cycle arrests and propagation of unrepaired chromosomal damage in cancer cell lines with wild-type p53. *Mol Carcinogen* 1998; **23**: 1–12.
23. Hung DT, Jamison TF, Schreiber SL. Understanding and controlling the cell cycle with natural products. *Chem Biol* 1996; **3**: 623–39.
24. Sackett DL, Bhattacharyya B, Wolff J. Local unfolding and the stepwise loss of the functional properties of tubulin. *Biochemistry* 1993; **33**: 12868–78.

(Received 27 April 2000; accepted 6 May 2000)